

Interplay between lattice, orbital, and magnetic degrees of freedom in the chain-polymer Cu(II) breathing crystals.

S.V. Streltsov,^{1,2} M.V. Petrova,³ V.A. Morozov,³ G.V. Romanenko,³ V.I. Anisimov,^{1,2} and N.N. Lukzen³

¹*Institute of Metal Physics, S.Kovalevskoy St. 18, 620990 Ekaterinburg, Russia*

²*Ural Federal University, Mira St. 19, 620002 Ekaterinburg, Russia**

³*International Tomography Center SB RAS, Institutskaya str. 3a, Novosibirsk, Russia*

(Dated: November 11, 2018)

The chain-polymer Cu(II) “breathing crystals” $C_{21}H_{19}CuF_{12}N_4O_6$ were studied using the X-ray diffraction and *ab initio* band structure calculations. We show that the crystal structure modification at $T=146$ K, associated with the spin crossover transition, induces the changes of the orbital order in half of the Cu sites. This in turn results in the switch of the magnetic interaction sign in accordance with the Goodenough-Kanamori-Andersen theory of the coupling between the orbital and spin degrees of freedom.

PACS numbers: 75.30.Wx, 61.66.Hq, 31.15.A-

I. INTRODUCTION

The conventional phenomenon of spin crossover (SCO) is a well-known change of the spin state observed in some octahedral coordinated transition metal complexes. [1] There are exist thermally, doping, photo- and pressure induced SCO transitions. [1–4]. In the classical case of Fe(II) complexes with d^6 electron configuration the thermal SCO involves a transition from the low spin state ($S=0$, t_{2g}^6) to the high spin state ($S=2$, $t_{2g}^4e_g^2$) [5, 6] at elevating temperature. The SCO compounds represent bright examples of a bistability in the molecular crystals[7] and are promising candidates for multifunctional materials[8] with potential applications to the memory devices, the optical, temperature and pressure sensors etc. [9]

Recently rather different SCO transitions were found in the chain-polymer compounds Cu(II) with nitroxides. [10] These compounds contain chains of the exchange clusters with two or three spins. The exchange clusters contain Cu^{2+} , ligands and some organic radicals. For the essential structural changes in the polyhedral surrounding Cu ions under the SCO transitions these compounds were called “breathing crystals”. [11] The main feature of the “breathing crystals” compounds is their ability to pass through reversible thermal induced structural transformations (often similar to phase transitions) accompanied by changes of magnetic susceptibility and optical properties. [12]. Note that one should not confuse the “breathing crystal” with the well known dynamical “breathing mode” – a specific collective excitation of confined systems of quantum [13] or classical [14] particles.

The classical SCO transition, associated with the change of spin state of single ion, is impossible for isolated d^9 centers of Cu(II) ($S=1/2$, $t_{2g}^6e_g^3$). Thus, the reason of

unusual spin transitions inherent in the Cu(II) complexes with nitroxides possibly arise from the change of the total electron spin of a whole exchange cluster.

Magnetic measurements show that the temperature induced SCO transition in one of the Cu(II) breathing crystals, characterized by the chemical formula $C_{21}H_{19}CuF_{12}N_4O_6$, is accompanied by the lost of the half of local spins. [11] This fact can be explained by the formation of spin singlets ($S=0$) in the half of the exchange clusters, but the reason for this is unknown.

The aim of our paper is to provide a microscopic description of the changes in the magnetic properties of $C_{21}H_{19}CuF_{12}N_4O_6$, often abbreviated as $Cu(hfac)_2 L^{Me}$ in the chemical literature. With the use of the density functional theory (DFT) we found that there is an interplay between the magnetic properties, orbital structure and lattice distortions in the “breathing crystals”. These correlations between different degrees of freedom results in the SCO transition at 146 K in the compound under consideration.

II. CRYSTAL STRUCTURE

The crystal structure of $C_{21}H_{19}CuF_{12}N_4O_6$ was solved from the X-ray single crystals diffraction data. The data were collected using a SMARTAPEXCCD (Bruker AXS) automated diffractometer with aHelix (Oxford-Cryosystems) open-flow helium cooler using the standard procedure (Mo K α radiation). The structures were solved by direct methods and refined by the full-matrix least-squares procedure anisotropically for non-hydrogen atoms. The H atoms were partially located in difference electron density syntheses, and the others were calculated geometrically and included in the refinement as riding groups. All calculations were fulfilled with the SHELXTL 6.14 program package.

Crystal data for the compound $Cu(hfac)_2 L^{Me}$ are the following: $C_{21}H_{19}CuF_{12}N_4O_6$, FW = 714.94, $T = 240/110$ K, triclinic crystals, space group

*Electronic address: streltsov@imp.uran.ru

P-1, $a=12.1987(9)/11.9560(9)\text{\AA}$, $b=15.5950(11)/15.0506(12)\text{\AA}$, $c=15.8716(11)/15.8657(12)\text{\AA}$, $\alpha = 84.459(2)/81.306(1)^\circ$, $\beta = 74.132(2)/76.943(2)^\circ$, $\gamma = 87.315(1)/85.502(1)^\circ$, $V = 2890.1(4)/2746.3(4)\text{\AA}^3$, $Z=4$, $D_{calc} = 1.643/1.729\text{ g/cm}^3$, $\mu = 0.875/0.921\text{ mm}^1$, 12570/11868 measured reflections ($\theta_{max} = 23.35/23.30^\circ$), 8291/7907 unique reflections ($R_{int} = 0.0293/0.0230$), 6043/6521 reflections with $I > 2\sigma_I$, 793/794 refined parameters; GOOF = 1.061/1.103, $R1 = 0.0598/0.0481$, $wR2 = 0.1500/0.1307$ ($I > 2\sigma_I$). The list of the atomic positions for T=240 K and T=110 K is given in the Supplemental Materials. [15]

The crystal structure of $C_{21}H_{19}CuF_{12}N_4O_6$ consists of the polymer chains running along b direction (Fig. 1) with a “head-to-tail” motif containing the exchange clusters of type $N\dot{O}-Cu^{2+}$. An isolated chain of the exchange clusters is presented in Fig. 2 with the F and H atoms being omitted for simplicity.

At high temperature (HT) phase the CuO_5N units are the elongated octahedra with Cu-O axial distance of $\sim 2.5\text{ \AA}$ and Cu-N distance of $\sim 2.3\text{ \AA}$. Equatorial distances Cu-O are about 1.95 \AA . With decrease of the temperature the compound undergoes the SCO transition in the vicinity of 150 K, which is accompanied by the substantial structural changes. As a result of the transition within a half of the CuO_5N octahedra the elongation direction changes. In the octahedra surrounding Cu1 ion two equatorial bonds with oxygens turn out to be the longest, while in the Cu_2O_5N octahedra the elongation direction still coincides with the O-Cu-N bond, like in the HT phase. Corresponding bond lengths can be found in Tab. I for the HT (240 K) and LT (110 K) phases.

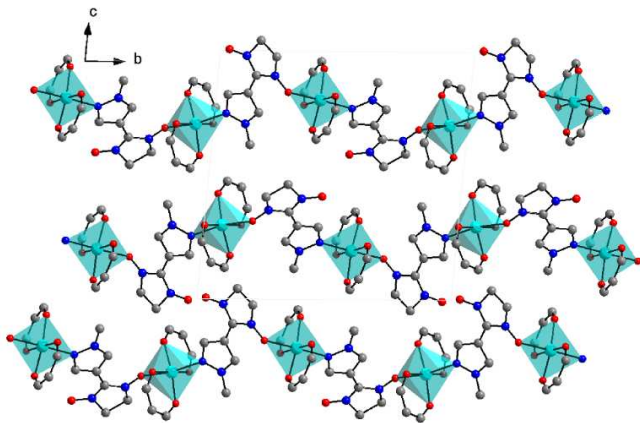


FIG. 1: . (Color online) The crystal structure of high temperature triclinic phase of the “breathing crystal” compound $C_{21}H_{19}CuF_{12}N_4O_6$. Turquoise balls are the Cu ions, red and blue balls are the O and N atoms. Grey balls are the C atoms. The fluorine atoms and the hydrogen atoms are omitted for clarity of the figure. Coordination units CuO_5N are marked with turquoise octahedra.

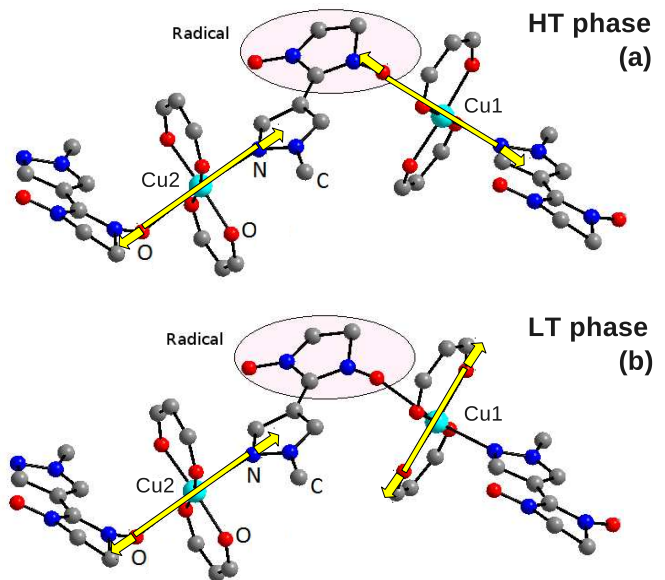


FIG. 2: . (Color online) The structure of isolated polymer chain of the “breathing crystal” compound $C_{21}H_{19}CuF_{12}N_4O_6$. The color coding is the same as in Fig. 1. The fluorine atoms and the hydrogen atoms are omitted for clarity of the figure. Methyl ligand characterizing this compound is marked by C. In other compounds of the “breathing crystals” family the ligand may be propyl or butyl type. A fragment of nitroxide radical with nonzero spin densities on atoms is marked with the oval. The direction of the CuO_5N octahedra elongation are shown by the yellow bars and arrows.

III. PREVIOUS CALCULATIONS OF THE “BREATHING CRYSTALS”

The first attempt to understand a nature of the spin exchange in the clusters containing the Cu atoms and a stable nitroxyl radical was performed rather far ago by Musin et al. [16] The authors provided a detail quantum-chemical analysis of the possible mechanisms of the exchange interaction in the magnetic fragments $Cu(II)\cdots O-\dot{N} < (or > \dot{N}-O\cdots Cu(II)\cdots O-\dot{N} <$) of bischelating complexes of Cu(II) with nitroxyl radicals. The drawback of this and some other [17–20] treatments was in the consideration of an isolated fragment rather than the crystal as a whole.

Till now the only consistent calculation of the electronic and magnetic properties of the “breathing crystals” was performed in Ref. 21, where the spin densities and the magnetic moments of a heterospin compound based Cu(II) hexafluoroacetylacetonate ($Cu(hfac)_2$; $hfac=CF_3-C(O)-CH-C(O)-CF_3$) in combination with a stable nitronyl nitroxide radical were calculated. This system is similar to the one of interest in the present paper, the difference is in another substitute in the position 1 of the pyrazol ring - the ethyl radical instead of the methyl one in our system. This difference

TABLE I: Bond distances of $\text{Cu}_2\text{O}_5\text{N}$ octahedra in \AA . The first four rows correspond to distances in the equatorial plane, i.e. perpendicular to the chain direction, while the last two ones to the axial direction (along the chain). The space group is the same P-1 for both phases.

Bond	HT phase	LT phase	Bond	HT phase	LT phase
	T=240 K	T=110 K		T=240 K	T=110 K
Cu1-O	1.95	1.97	Cu2-O	1.93	1.85
Cu1-O	1.95	2.16	Cu2-O	1.95	1.85
Cu1-O	1.96	1.98	Cu2-O	1.96	1.97
Cu1-O	1.97	2.23	Cu2-O	1.97	1.97
Cu1-O	2.49	1.99	Cu2-O	2.49	2.42
Cu1-N	2.30	2.02	Cu2-N	2.32	2.32

results in another organization of the polymer chain: in the case considered in Ref. ? the chain of the exchange clusters has “head-to-head” coupling of the ligands to the magnetic Cu atoms embedded in $(\text{hfac})_2$ blocks, while in the present case the chain motif is “head-to-tail”.

Thus, in Ref. 21 the corresponding chain contains “three spin - isolated spin” structure, while in the case considered in the present paper the chain is composed of two spin clusters. This results in a different magnetic properties. It should also be mentioned that in Ref. 21 only a high temperature phase of the crystal was calculated. At the same time both high-temperature and especially low temperature phase represent a great interest for study of phase transitions.

IV. CALCULATION DETAILS

The pseudo-potential PW-SCF code was used for the band structure calculations. [22] We utilized ultrasoft pseudo-potentials with nonlinear core correction (for better description of the magnetic interactions) with Perdew-Burke-Ernzerhof (PBE) version of the exchange-correlation potential. [23] The charge density and kinetic energy cut-offs equal 35 Ry and 180 Ry, respectively. The integration in the k-space in the course of the self-consistency was performed over the mesh of 4 k-points in the Brillouin zone using gaussian smearing of 13.6 meV. The density of states was calculated with the smearing of 40.8 meV.

The correlations on Cu sites were taken into account within the frameworks of the GGA+U approximation (generalized gradient approximation with account of on-site Coulomb repulsion). [24] The intra-atomic exchange interaction J_H and on-site Coulomb repulsion parameters for Cu^{2+} ions were chosen to be 0.9 and 7.0 eV respectively [25, 26].

The calculations were performed for the experimentally measured crystal structure, presented in Ref. 15 However, in order to decrease the number of atoms in the unit cell (from 252 to 126) we used P1 instead of the

TABLE II: The results of the GGA+U calculation for two different crystal structures corresponding to the temperatures $T=110$ K (LT) and $T=240$ K (HT) and to the FM and AFM types of magnetic order of the Cu spins. All the values are in μ_B units. The total and absolute (abs) magnetization are per unit cell.

	HT phase	HT phase	LT phase	LT phase
	FM	AFM	FM	AFM
total magn.	3.92	0.06	2.00	2.00
abs magn.	4.40	4.44	4.07	4.07
moment Cu1	0.52	-0.52	0.45	-0.45
moment Cu2	0.55	0.55	0.55	0.55

P-1 space group. The inversion center in the P-1 space group produces additional chains, so that reducing the crystal symmetry we neglect the interchain interactions. This seems to be a reasonable approximation, since the main changes in the crystal structures at the SCO transition occur within a chain.

V. CALCULATION RESULTS

A. High-temperature phase

We start with the calculations of the HT phase. The compound under consideration experimentally is known to be paramagnetic. [11] However, in any band structure calculation the translational symmetry is assumed, so that one may calculate the ferromagnetic (FM), when both Cu ions in the unit cell (u.c.) have the same spin direction, antiferromagnetic, with the opposite spins on the neighboring Cu atoms, or non-magnetic, when up and down spins on all ions are equally populated. It’s clear that the non-magnetic configuration is the worst approximation, since there must be local magnetic moments in the paramagnetic insulator. In the following we will investigate the FM and AFM solutions, which actually provide very similar results since magnetic ions (Cu) are quite far a way from each other.

Indeed, the absolute values of the magnetic moments on two Cu ions were found to be $0.52 \mu_B$ and $0.55 \mu_B$, the same for the FM and AFM solutions (see Tab. II). They differ from $1 \mu_B$ expected for the isolated Cu^{2+} ions due to a strong hybridization with ligands and formation of a molecular orbital on which a single hole in the $3d$ shell of the Cu^{2+} ion is localized. This molecular orbital (or the Wannier orbital) has the contributions of the Cu d and ligand p orbitals, so that the spin moment on the whole molecular orbital should be $1 \mu_B$, but the part of the spin density projected on the Cu $3d$ states provides only a part of it. This is clearly seen from the density of states plot presented in Fig. 3. The peak at ~ 0.1 eV corresponding to a single hole in the Cu $3d$ shell shows significant contribution coming from the O $2p$ states. Another illustration of the considerable mixing between Cu

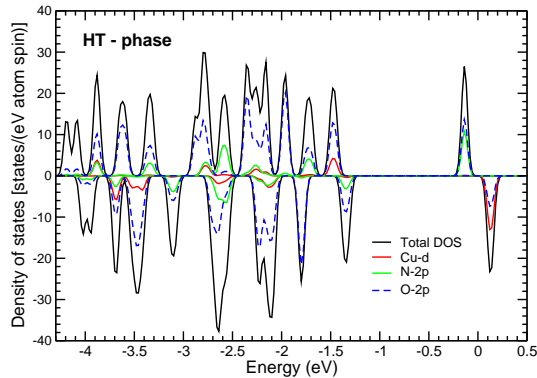


FIG. 3: . Results of the GGA+U calculation for the high temperature phase, where the spins on different Cu ions are ferromagnetically ordered. Positive (negative) values correspond to the spin up (down). The gaussian smearing 0.04 eV was used. The Fermi energy is set to zero.

$3d$ and O $2p$ states can be found in Figs. 5 and 6, where the spin density plot for the LT phase is presented.

It is useful to proceed with the analysis of the total magnetization per unit cell defined as $m_{tot} = \sum_i m_i$, where $m_i = g\mu_B s_i$ is the magnetization on the i th atom, and s_i – its spin moment. The total magnetization equals $3.92\mu_B$ in the FM and $0.06\mu_B$ in the AFM configuration. Since there are two pairs radical-Cu in the unit cell, it means that at least in the FM configuration the spins on the radicals are *parallel* to the spin moment of the molecular orbital on the neighboring (to this radical) Cu ion. The spin density projection shows that the largest moment on p -elements (O, C, F, and N) are indeed parallel to the moments of Cu. The values of the largest moments ($>0.1\mu_B$) in the case of the FM order are the following: O10 ($0.24\mu_B$); O11 ($0.30\mu_B$); O12 ($0.31\mu_B$); N1,N2,N5 ($0.22\mu_B$); N6 ($0.22\mu_B$).

In other words the pair radical-Cu is in the triplet ground state ($S=1$, where S is the spin of the pair). The deviation from the $4\mu_B$ for the FM and from $0\mu_B$ for the AFM solutions is attributed to the sparse mesh in the k -space, used to integrate energy bands in such a large unit cell, consisting of 126 atoms.

In principle one may explain the ferromagnetic coupling (parallel spin arrangement) of the spins on the Cu ions and radicals in two ways. First of all one may argue that the local spin on Cu simply magnetizes all the surrounding ions. Microscopically this means that due to a strong hybridization the Zeeman (spin) splitting in the Cu $3d$ shell spreads out on the s and p shells of the neighboring ligands. However, this picture is too simplified and doesn't take into account the details of the electronic structure of the compound under consideration and is unable to explain the antiferromagnetic coupling between Cu and the radical which is observed at low tem-

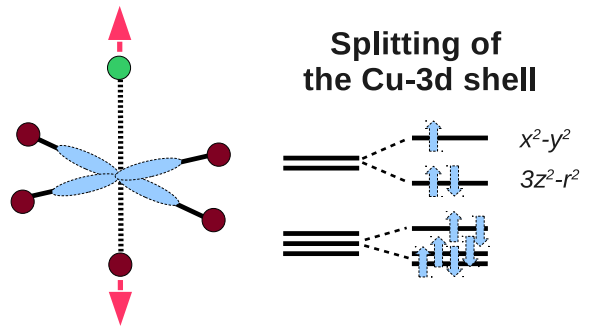


FIG. 4: . (Color online) The sketch of the local distortion of CuO_5N octahedra (oxygen and nitrogen atoms are brown and green balls, respectively) in the high temperature phase. The direction of the distortion is shown by the red arrows. The elongation of the octahedra leads to the stabilization of a hole on the $x^2 - y^2$ orbital.

peratures and will be discussed latter. Therefore below we present the model, which explains in details how the magnetic coupling with the radicals is related to the local lattice distortions and the orbital structure of the Cu- $3d$ shell.

According to the crystal structure analysis presented above in Sec. II the distortions of both CuO_5N octahedra (which belong to the same unit cell) are quite similar. Since the Cu^{2+} ion is Jahn-Teller active, both octahedra are strongly distorted. They are elongated in the direction of the O-Cu-N bond. The average Cu-O distance in the equatorial plane is $\sim 1.95\text{\AA}$, while the bond lengths with the apical ligands are ~ 2.30 and 2.49\AA , for the Cu-O and Cu-N bonds respectively.

Such a distortion of the local surrounding of the Cu^{2+} leads to a certain splitting in the e_g shell of these ions: the orbital of the $x^2 - y^2$ symmetry turns out to be higher in energy than $3z^2 - r^2$, as it is shown in Fig. 4. As a result the hole localizes on this $x^2 - y^2$ molecular orbital, which lies in the plane orthogonal to the bond with the radical. By symmetry this orbital may hybridize only with the O $2p$ states, not with the N $2p$ orbitals. This is clearly seen in Fig. 3, where the peak corresponding to the hole states at $\sim 0.1\text{ eV}$, does not have the contribution coming from the N $2p$ states.

Thus the overlap between magneto-active orbital centered on the Cu^{2+} ion and the molecular orbital bearing the local spin on the radical is negligible. The only possible magnetic coupling between Cu and the radical is via orbital of the $3z^2 - r^2$ symmetry. But this interaction between the completely filled $3z^2 - r^2$ orbital and the partially filled radical molecular orbital must be ferromagnetic according to famous Goodenough-Kanamori-Andersen (GKA) rules. [27] This is exactly what we observe in the calculation.

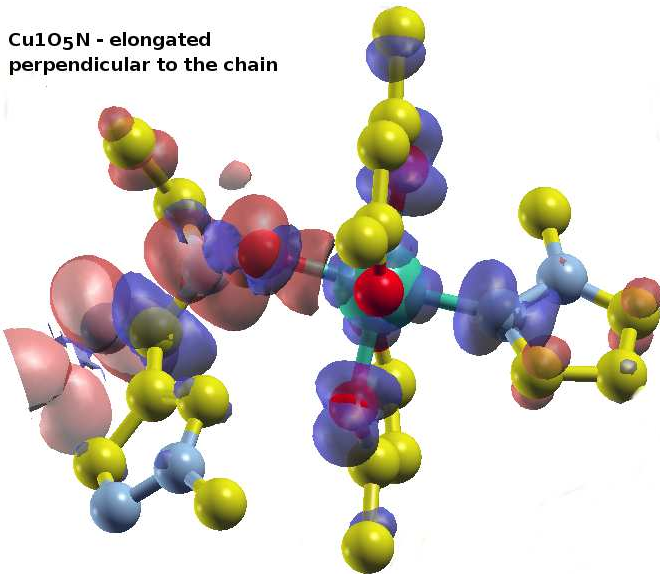


FIG. 5: . (Color online) The spin density ($\rho^\uparrow(\vec{r}) - \rho^\downarrow(\vec{r})$) in the vicinity of the Cu1 ion obtained in the GGA+U calculation for LT phase. The Cu, N, O and C ions are shown as light green, light blue, red and yellow balls correspondingly. The parts of the spin density, which have different signs are painted by different colors: brown and violet. Thus, one may easily see that the spins on the radical and on the Cu1 are antiparallel. The plot is for the FM order of Cu spins, but the AFM order gives qualitatively the same.

B. Low-temperature phase

The situation in the low temperature (LT) phase is more complicated, mainly due to the change in the direction of the elongation in a half of the CuO₅N octahedra. In the LT phase the octahedra surrounding the Cu1 ions turn out to be elongated not in the direction of the chain, but perpendicular to it. This is schematically shown in the Fig. 2(b). The change of the elongation direction results in the rotation of the single magneto-active orbital on the Cu1 ion. The symmetry of this orbital must be the same, $x^2 - y^2$, (here we used the notations of the local coordinate system, where z -axis corresponds to elongation direction), but two lobes of the orbital must point to the radical.

In the Fig. 5 the spin density (difference between the charge densities for two spin projections) around the Cu1 ion obtained in the GGA+U calculation is shown. In the case of the Cu²⁺ (d^9) this corresponds to the spatial distribution of the single unoccupied orbital. One may see that as it was described in details in the previous section the single hole is actually stabilized not on the atomic, but on the molecular (Wannier) orbital, which has significant contribution on the neighboring ligands. The symmetry of the orbital is $x^2 - y^2$, but it is pointed exactly at the spin density centered on the radical (left part of the Fig. 5). The strong overlap between the half-filled orbitals centered on the Cu1 ion and on the radical re-

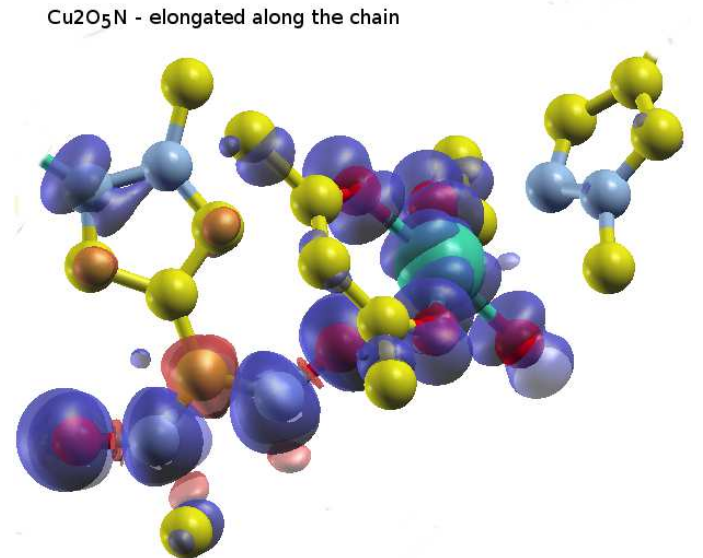


FIG. 6: . (Color online) The spin density ($\rho^\uparrow(\vec{r}) - \rho^\downarrow(\vec{r})$) in the vicinity of the Cu2 ion obtained in the GGA+U calculation for LT phase. The Cu, N, O and C ions are shown as light green, light blue, red and yellow balls correspondingly. The parts of the spin density, which have different signs are painted by different colors: brown and violet. Thus, the spins on the radical and on the Cu2 are parallel. The plot is for the FM order of Cu spins, but the AFM order gives qualitatively the same.

sults in the strong antiferromagnetic coupling $J \sim 2t^2/U$ according to the GKA rules. [27] Here t is the hopping integral and U - the on-site Coulomb repulsion parameter. The fact that this super-exchange interaction in the real calculation does lead to the antiferromagnetic order of the spins on the radical and Cu1 is clearly seen from the Fig. 5. The signs of the spin density on these two objects are indeed different.

The presence of the molecular orbital centered on the radical with the spin antiparallel to the spin on one of the Cu ions is also seen in Fig. 7. In contrast to the HT phase there are two peaks above the Fermi level. One of them has contributions coming from the Cu $3d$, N $2p$ and O $2p$ states, while another only from the N $2p$ and O $2p$ states. The last one has the spin projection opposite to the spins on the Cu ions.

The spin density centered on the Cu2 ion is presented in Fig. 6. One may see that it is concentrated in the plane perpendicular to the charge density of the radical (so called antiferro-orbital ordering). This leads to the FM coupling between Cu2 and the neighboring radical, as in the HT phase according to the GKA rules. Indeed the sign of the spin density is the same on the radical and on the Cu2 ion.

The fact that there must be a different magnetic coupling in two pairs Cu-radical in the LT phase according to the charge density analysis is also seen from the values

spins in the low temperature phase. [11]

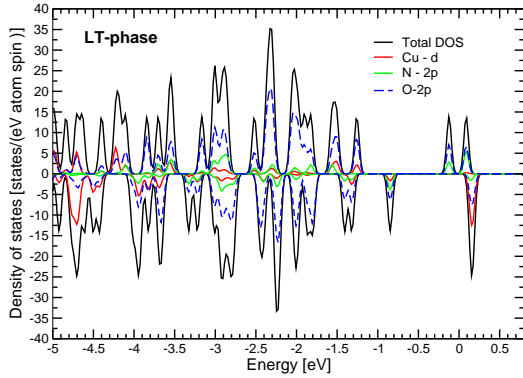


FIG. 7: . Results of the GGA+U calculation for the low temperature phase, where the spins on different Cu ions are ferromagnetically ordered. Positive (negative) values correspond to the spin up (down). The gaussian smearing 0.04 eV was used. The Fermi energy is set to zero.

of the total and absolute magnetic moments per unit cell. The total magnetic moment per unit cell is the same, $2.0 \mu_B$ in both FM and AFM configurations, which shows that there is one pair of electrons on the Cu^{2+} ion and the radical with the parallel spin direction and another one with the antiparallel spins. The fact that the absolute magnetization defined as $m_{abs} = \sum_i |m_i|$ is equal to $4.07 \mu_B$ additionally supports this interpretation.

The absolute values of magnetic moments were found to be the same in the FM and AFM solutions and equal to $0.45 \mu_B$ and $0.55 \mu_B$ for the Cu1 and Cu2 ions respectively (a difference in the values of magnetic moments as compare to the high temperature phase can be connected with a slightly different hybridization with ligands, due to different Cu-O(N) distances).

The strong antiferromagnetic coupling results in the spin singlet state ($S=0$) formation in the Cu1 exchange clusters for which the CuO_5N octahedra are elongated perpendicular to chain direction. This is exactly what is observed experimentally - the lost of the half of localized

VI. CONCLUSIONS

We present a microscopic theory, which describes anomalous changes of the magnetic properties of $\text{C}_{21}\text{H}_{19}\text{CuF}_{12}\text{N}_4\text{O}_6$ “breathing crystal” through the coupling between the spins and another degrees of freedom such as orbital and lattice.

With the use of the *ab initio* band structure calculations we show that the change of the crystal structure of $\text{C}_{21}\text{H}_{19}\text{CuF}_{12}\text{N}_4\text{O}_6$ with decrease of the temperature results in the rotation of the half-filled orbital of one of the Cu^{2+} ions in the unit cell. The $x^2 - y^2$ orbital lies in the plane orthogonal to the O-Cu-N bond and provides ferromagnetic coupling at the high temperatures. With decrease of temperature the distortions of the half of the CuO_5N octahedra are changed, so that two lobes of the $x^2 - y^2$ orbital on the Cu1 sites turn out to be directed along the O-Cu-N bond. This leads to a strong antiferromagnetic coupling and stabilization of the spin singlet ($S=0$) state in the half of the exchange clusters at lower temperatures. As a result only a half of local spins of the compound turns out to be unpaired and the value of observed effective magnetic moment drastically drops. [11, 20]

VII. ACKNOWLEDGMENTS

The authors are thankful to Prof. V.I. Ovcharenko for his useful comments. This work is supported by the Russian Foundation for Basic Research via MK-3443.2013.2, RFFI-10-02-96011, RFFI-13-02-00374, RFFI-10-03-00075 and RFFI-10-02-00140, the Ministry of education and science of Russia (grants 12.740.11.0026 and 8436), by the Ural branch of Russian Academy of Science through the young-scientist program. shown in this document. All the calculation were performed on the “Uran” cluster of the IMM UB RAS.

-
- [1] P. Gütllich and H. A. Goodwin, *Spin Crossover in Transition Metal Compounds I, II, and III*, Topics in Current Chemistry (Springer, 2004), ISBN 9783540403951, URL http://books.google.ru/books?id=rNkQ_Ddiowc.
- [2] N. A. Babushkina, A. N. Taldenkov, S. V. Streltsov, T. G. Kuzmova, A. A. Kamenev, A. R. Kaul, D. I. Khomskii, and K. I. Kugel, to be published (2012).
- [3] Y. Ogawa, S. Koshihara, K. Koshino, T. Ogawa, C. Urano, and H. Takagi, *Phys. Rev. Lett.* **84**, 3181 (2000), ISSN 1079-7114, URL <http://www.ncbi.nlm.nih.gov/pubmed/11019042>.
- [4] H. J. Shepherd, S. Bonnet, P. Guionneau, S. Bedoui, G. Garbarino, W. Nicolazzi, A. Bousseksou, and G. Molnár, *Phys. Rev. B* **84**, 144107 (2011), ISSN 1098-0121, URL <http://link.aps.org/doi/10.1103/PhysRevB.84.144107>.
- [5] S. V. Streltsov and N. A. Skorikov, *Phys. Rev. B* **83**, 214407 (2011), ISSN 1098-0121, URL <http://link.aps.org/doi/10.1103/PhysRevB.83.214407>.
- [6] A. Hauser, *Topics in Current Chemistry* **234** (2004).
- [7] S. Cobo, D. Ostrowskii, S. Bonhommeau, G. Molnar, L. Salmon, K. Tanaka, and A. Bousseksou, *Topics in Current Chemistry* **130**, 9019 (2008).
- [8] P. Gütllich, A. Hauser, and H. Spiering, *Angewandte Chemie International Edition in English* **33**, 2024 (1994), ISSN 0570-0833, URL

- <http://doi.wiley.com/10.1002/anie.199420241>.
- [9] J. F. Létard, P. Guionneau, and L. Goux-Capes, *Topics in Current Chemistry* **235**, 221 (2004).
- [10] V. I. Ovcharenko, S. V. Fokin, G. V. Romanenko, V. N. Ikorskii, E. V. Tretyakov, S. F. Vasilevsky, and R. Z. Sagdeev, *Mol. Phys.* **100**, 1107 (2002).
- [11] V. I. Ovcharenko, K. Maryunina, S. V. Fokin, E. V. Tretyakov, G. V. Romanenko, and V. N. Ikorskii, *Russ. Chem. Bull.* **53**, 2406 (2004).
- [12] E. V. Tretyakov, S. E. Tolstikov, A. O. Suvorova, A. V. Polushkin, G. V. Romanenko, A. S. Bogomyakov, S. L. Veber, M. V. Fedin, D. V. Stass, E. Reijerse, et al., *Inorganic chemistry* **51**, 9385 (2012), ISSN 1520-510X, URL <http://dx.doi.org/10.1021/ic301149e>.
- [13] J. W. Abraham, K. Balzer, D. Hochstuhl, and M. Bonitz, *Physical Review B* **86**, 125112 (2012), ISSN 1098-0121, URL <http://link.aps.org/doi/10.1103/PhysRevB.86.125112>.
- [14] A. Olivetti, J. Barré, B. Marcos, F. Bouchet, and R. Kaiser, *Physical Review Letters* **103**, 224301 (2009), ISSN 0031-9007, URL <http://link.aps.org/doi/10.1103/PhysRevLett.103.224301>.
- [15] See *Supplemental Material at [URL] for the list of the atomic positions for $T=240$ K and $T=110$ K*.
- [16] R. N. Musin, P. V. Schastnev, and S. A. Malinovskaya, *Inorg. Chem.* **31**, 4118 (1992).
- [17] V. Ovcharenko, G. V. Romanenko, K. Y. Maryunina, A. Bogomyakov, and E. V. Gorelik, *Inorg. Chem.* **47**, 9537 (2008).
- [18] E. M. Zueva, E. R. Ryabykh, and A. M. Kuznetsov, *Russian Chemical Bulletin* **58**, 1654 (2010), ISSN 1066-5285, URL <http://www.springerlink.com/index/10.1007/s11172-009-02>
- [19] S. Vancoillie, L. Rulísek, F. Neese, and K. Pierloot, *The journal of physical chemistry. A* **113**, 6149 (2009), ISSN 1520-5215, URL <http://www.ncbi.nlm.nih.gov/pubmed/19413285>.
- [20] M. V. Fedin, S. L. Veber, K. Y. Maryunina, G. V. Romanenko, E. A. Suturina, N. P. Gritsan, R. Z. Sagdeev, and E. G. Ovcharenko, V. I. Bagryanskaya, *J. Am. Chem. Soc.* **132**, 13886 (2010).
- [21] A. V. Postnikov, A. V. Galakhov, and S. Blügel, *Phase Transitions* **78**, 689 (2005), ISSN 0141-1594, URL <http://www.tandfonline.com/doi/abs/10.1080/014115905002>
- [22] P. Giannozzi, S. Baroni, N. Bonini, M. Calandra, R. Car, C. Cavazzoni, D. Ceresoli, G. L. Chiarotti, M. Cococcioni, I. Dabo, et al., *J. Phys.: Condens. Matter* **21**, 395502 (2009).
- [23] J. P. Perdew, K. Burke, and M. Ernzerhof, *Phys. Rev. Lett.* **77**, 3865 (1996), ISSN 1079-7114, URL <http://www.ncbi.nlm.nih.gov/pubmed/10062328>.
- [24] V. Anisimov, F. Aryasetiawan, and A. Lichtenstein, *J. Phys.: Condens. Matter* **9**, 767 (1997), URL <http://iopscience.iop.org/0953-8984/9/4/002>.
- [25] A. I. Liechtenstein, V. I. Anisimov, and J. Zaanen, *Physical Review B* **52**, 5467 (1995), URL http://prola.aps.org/abstract/PRB/v52/i8/pR5467_1.
- [26] S. V. Streltsov and D. I. Khomskii, *Phys. Rev. B* **86**, 035109 (2012).
- [27] J. B. Goodenough, *Magnetism and the Chemical Bond* (Interscience-Wiley, 1963).